

# Particle Acceleration in Relativistic Flows

J. G. Kirk

Max-Planck-Institut für Kernphysik, 69029 Heidelberg, Germany

A property common to several different astrophysical sources of high-energy gamma-rays is the presence of bulk motion at relativistic speed. The intrinsic spectra of the nonthermal radiating particles also show interesting similarities, with a pronounced hardening towards lower energies. This suggests two distinct acceleration mechanisms could be at work in these sources. At high energies, the stochastic first-order Fermi process at shocks seems to provide a reasonable explanation. I will briefly review the status of this mechanism before discussing the possibility that, at lower energies, non-stochastic acceleration in the induced electric field of a relativistic current sheet plays a role.

## 1. INTRODUCTION

With only one or two exceptions, the identification of relativistic bulk motion in an astrophysical source rests on the interpretation of its nonthermal radiation — normally a featureless continuum, presumably produced by relativistic electrons as either synchrotron radiation or by the inverse Compton scattering mechanism. This makes it very difficult to constrain the underlying physics. In most cases, cut-off or break frequencies are only poorly defined by the data and the only quantity that can be used to constrain models is a spectral index. Even this is not always easy to interpret: to be meaningful, it requires a power-law spectrum extending over at least a couple of decades in frequency. Nevertheless, the evidence accumulated from the spectra of shocked pulsar winds, gamma-ray bursts, and blazars indicates that the distribution of radiating particles is relatively soft at high energy ( $s = -d \ln f / d \ln \gamma \gtrsim 4$ , where  $f$  is the phase-space density of the injected particles) and hard at low frequencies ( $s \lesssim 3.6$ ). The first-order Fermi mechanism operating at a relativistic shock predicts indices not too different from those seen at high energies, but it fails to provide an explanation for the hard low energy spectra. A promising candidate mechanism in this regime appears to be acceleration at current sheets. In this paper I briefly discuss the observational evidence, review the predictions of the first-order Fermi mechanism and summarise recent ideas on relativistic current sheets.

## 2. OBSERVATIONS

Plerions — filled-centre supernova remnants [Weiler and Panagia 1978] — are thought to contain a pulsar that powers the nonthermal nebular emission within the supernova bow-shock via a magnetised, relativistic wind. Although data on the spectra of several examples have been modelled [e.g., Chevalier 2000], by far the best observed member of this class is the Crab Nebula. Optical and X-ray images of this object show features that apparently move with

mildly relativistic velocities  $\sim 0.5c$  [Hester *et al.* 2002]. However, an analysis of the dynamics of the pulsar wind responsible for the powering of the Nebula indicates that it is highly relativistic (bulk Lorentz factor  $\Gamma \sim 10^3$  to  $10^6$ ) and may also be strongly magnetised [Kennel and Coroniti 1984, Kundt and Krotscheck 1980, Lyubarsky and Kirk 2001, Lyubarsky 2003, Rees and Gunn 1974]. Over the entire X-ray energy range  $2 \times 10^{16}$  to  $6 \times 10^{20}$  Hz its spectrum is well-described by a power-law of photon index  $q = -d \ln N_\gamma / d \ln \nu = 2.11$  [Massaro *et al.* 2000]. In the gamma-ray region, this synchrotron spectrum cuts off at around  $10^{22}$  Hz, whereas towards lower frequencies it hardens substantially, reaching a photon index of  $q = 0.26$  in the radio range ( $10^8$  to  $10^{10}$  Hz), [Baars and Hartsuijker 1972, Bietenholz and Kronberg 1992].

In the case of gamma-ray bursts, there is a general consensus that a highly relativistic flow with large Lorentz factor  $\Gamma \gtrsim 100$  is present. Nevertheless, it is difficult to constrain the physics of the outflow with the available data. Several break frequencies are predicted, and have been identified in the observations [for a review see Piran 2005]. But direct observation of a power-law spectrum over a substantial frequency range is elusive. The “measured” indices frequently represent interpolations between observation bands. Light curves are in some cases quite accurately known, but can only be used to constrain theories of the acceleration mechanism when combined with additional assumptions about the dynamics of the expansion. Nevertheless, all models currently discussed conform to the trend of a hard electron spectrum at low energy (usually manifested as a low energy cut-off) and a softer one at high energy, although in some bursts, even the X-ray synchrotron emission may lie in the “low energy” regime according to this definition [Moran *et al.* 2005].

A third class of object thought to harbour a relativistic flow is that of blazars. Relativistic bulk speeds are required both to explain apparently superluminal motion in their jets and by the rapid variability in their gamma-ray spectra. As in the case of gamma-ray bursts, the spectra do not show clean

power-law behaviour over several decades of photon energy but demand a detailed analysis before they can be interpreted in terms of acceleration theory [Sambruna *et al.* 1996, Tavecchio *et al.* 2002]. At radio frequencies, the spectra are systematically harder than at high frequencies. This could either reflect the intrinsic particle distribution [Mastichiadis and Kirk 1997] or be caused by internal absorption. Several individual multi-frequency flares have been successfully modelled by using either a very hard injection spectrum  $s \approx 3.3$  combined with a high frequency cut-off [Konopelko *et al.* 2003] or a low frequency cut-off and softer  $s \approx 4.2$  high-energy power-law [Krawczynski *et al.* 2002].

The study of Blazar spectra illustrates the difficulties involved in trying to extract the intrinsic injected particle spectrum from an observed photon spectrum that has been shaped by various loss processes and by internal and possibly external absorption. An interesting alternative approach to this problem has recently been adopted for FR I radio galaxies by Young *et al.* [2005], who identify  $s = 4.1$  as a characteristic power-law index of the acceleration process. This analysis provides no evidence that the low energy particle distribution hardens, but cannot be interpreted as evidence against such a trend.

### 3. RELATIVISTIC SHOCKS

The first-order Fermi mechanism of particle acceleration at relativistic shocks rests on the assumption that energetic, charged particles are transported stochastically through the background plasma around a shock front [for a review see Kirk and Duffy 1999]. Particles cannot be assumed to “diffuse” in space. This is because the diffusion equation can be derived only for particles whose angular distribution function is approximately isotropic in the local plasma rest frame — an impossible requirement if the relative speed of the upstream and downstream plasmas is comparable to the speed of the particles themselves [Kirk and Schneider 1987], as, for example, at a relativistic shock.

Nevertheless, provided the particle transport process is stochastic and does not introduce a characteristic momentum scale into the problem, one can still expect the acceleration process to produce a power-law spectrum in particle energy, at least for ultra-relativistic particles, whose velocity can be considered to be independent of energy. A model of the transport process has to be adopted in order to find the power-law index, but the result appears to be rather insensitive to the particular choice. The kinematic problem of particle acceleration at a relativistic shock, i.e., that of finding the distribution of a collection of test particles undergoing small-angle, random, elastic (in the plasma frame) deflections in the vicinity

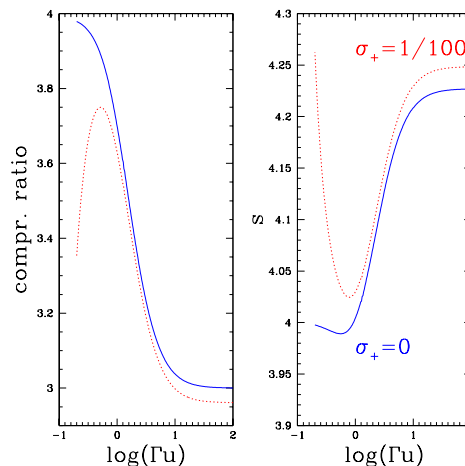


Figure 1: The power-law index  $s$  and the compression ratio of relativistic shocks as a function of the spatial component of the four-velocity of the upstream plasma into the shock  $\Gamma u$ . Two cases are shown: (i) non-magnetised with the full Sygne/Jüttner equation of state (solid line) and (ii) unmagnetised upstream (dotted line) but with an oscillating field component generated to the level of  $\sigma_+ = 1/100$  (see text).

of a discontinuity in the (relativistic) plasma velocity is well-understood. An analytic method based on an eigenfunction decomposition is available which gives the spectrum and angular dependence of the distribution function at energies well above those of injection for arbitrary shock speeds [Kirk *et al.* 2000]. In addition, Monte-Carlo simulations have been performed [Achterberg *et al.* 2001, Bednarz and Ostrowski 1998] finding good agreement with the analytic results. These are illustrated in Fig. 1 which shows the compression ratio and the high-energy power-law index  $s$  as a function of the spatial component of the 4-speed  $\Gamma u$  of the upstream plasma, where  $\Gamma = (1 - u^2)^{-1/2}$ . An interesting aspect of these results is that the power-law index tends asymptotically to the value  $s \approx 4.23$  for large shock Lorentz factors (or, equivalently, upstream Lorentz factors), independent of the equation of state of the plasma. This asymptotic value is essentially fixed by the compression ratio of the shock and depends only weakly on the form of the scattering operator used to describe the small-angle deflections.

The eigenfunction expansion method enables the full angle dependence of the distribution to be extracted, giving additional insight into the kinematics of the acceleration process. Both upstream and at the shock front itself the angular dependence is well-approximated by the simple expression

$$f \propto (1 - \mu_s u)^{-s} \exp\left(-\frac{1 + \mu_s}{1 - \mu_s u}\right) \quad (1)$$

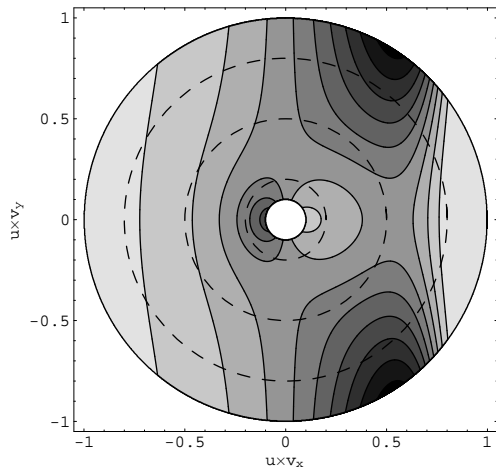


Figure 2: Contour plot of the approximate angular dependence of accelerated particles upstream of the shock front (Eq. 1 for  $s = 4.23$ ), plotted in the rest frame of the shock.  $v_x$  and  $v_y$  specify the particle velocity, and  $u$  is the three-speed of the background plasma flow, (which is in the positive  $x$  direction in this frame) in units of  $c$ . Since  $v_x^2 + v_y^2 = 1$  for ultra-relativistic particles, the angular distribution for given  $u$  lies on a circle of radius  $u$  (shown as dashed lines for  $u = 0.2, 0.5$  and  $0.8$ ). The contours are linear, starting at  $f = 0.1$  (light) and spaced by  $0.1$  up to  $f = .8$  (dark).

where  $\mu_s$  is the cosine of the angle between the shock normal and the particle velocity, measured in the frame in which the shock is at rest and the upstream plasma flows along the shock normal at speed  $c\vec{u}$ .

This function is illustrated in Fig. 2 for  $s = 4.23$ . Contours of  $f$  are shown as a function of a combination of the particle velocity components  $v_x$  and  $v_y$  and the speed of the upstream plasma into the shock  $u$ . The shock normal lies along the  $x$  axis, along which the plasma flows. Particles with  $v_x > 0$  are streaming back towards the shock front; the distribution is rotationally symmetric about the  $x$  axis. The further one goes away from the shock into the upstream region the better  $f$  approximates the full distribution. For ultra-relativistic shocks,  $f$  is a good approximation even at the shock front itself, in which case those particles with  $v_x > 0$  are crossing from upstream to downstream and those with  $v_x < 0$  vice versa. For a given upstream plasma speed  $u$ , the angular distribution of the accelerated particles is determined by the contours intersecting the circle of radius  $u$ , centred on  $v_x = v_y = 0$ . At low shock speeds, the distribution function is more or less isotropic, with a slight forwards/backwards asymmetry. However, above roughly  $u = 0.5$ , a pronounced cone emerges, directed back towards the shock front. In the ultra-relativistic limit, this cone has an opening (half) angle

$\theta_c$  given by

$$\theta_c = \arccos\left(\frac{s-2}{s}\right) \quad (2)$$

It is independent of the details of the upstream transport, provided these can be described as a diffusion in angle. The details of the downstream transport enter only in that they have a slight influence on the power-law index  $s$ . The cone arises because of two competing physical effects. Firstly, those particles that cross the shock with velocity inside the cone:  $v_x > \cos \theta_c$  are depleted because they have a high probability of escape downstream. Secondly, the angle at which a particle propagates in the upstream plasma reflects the energy and, to some degree, also the angle at which it last emerged from the downstream plasma. Figure 2 shows the upstream distribution at fixed energy in the shock rest frame. In this case, the higher  $v_x$ , the greater the energy gain has been since the last crossing. A large energy gain also implies that the potential source particles are more numerous. Consequently, this effect leads to a steady increase in the distribution function as  $v_x$  increases.

Using a Monte-Carlo approach, it is possible to investigate more general forms of the scattering operator, whilst retaining the effect of a non-vanishing average magnetic field [Achterberg *et al.* 2001, Ostrowski 1993, Virtanen and Vainio 2005]. Provided the turbulence remains strong, little difference is found. However, as expected, the acceleration mechanism becomes less effective as the turbulence diminishes [Ostrowski and Bednarz 2002], because the regular component of the field in the downstream region quickly drags particles away from the shock front [Begelman and Kirk 1990]. Explicit calculations of particle motion in a completely random magnetic field (with vanishing average component) have been performed by Ballard and Heavens [1992] and Casse *et al.* [2002]. They have been used to compute the acceleration around a relativistic shock for Lorentz factors  $\Gamma \leq 5$  [Ballard and Heavens 1992] and, more recently, for  $\Gamma \leq 100$  [Lemoine and Pelletier 2003]. The latter find good agreement with the analytic result on the asymptotic power-law index.

Although particle transport in astrophysical plasmas is usually dominated by interaction with fluctuations in the electromagnetic field produced collectively by the background plasma, there are strong indications that two-body *collisional* processes (including those with the photon gas e.g., photo-pion production and Compton scattering) may be important for the acceleration and/or the thermalisation of energetic particles in the inner parts of a GRB fireball  $r < 10^{16}$  cm [Derishev *et al.* 2003, Stern 2003]. These generically produce much harder spectra, principally because an energetic particle occasionally takes on an uncharged “identity” as a photon or neutron. This

facilitates flights deep into the upstream region, enabling the particle to profit from an energy boost of a factor  $\Gamma^2$ , which is normally available to charged particles only on their initial shock encounter. However, a hard spectrum enhances the modification of the shock front by the accelerated particles. This implies that fully nonlinear calculations will be required to assess the importance of collisional processes.

On the other hand, the nonlinear modification of a collisionless relativistic shock does not affect the *asymptotic* power-law index. There are two reasons for this: firstly, isotropised, accelerated particles behave like a relativistic gas with adiabatic index  $4/3$ , so that the overall compression ratio of an ultra-relativistic shock front remains 3, even when a significant part of the overall energy and momentum flux is carried by these particles. Secondly, the asymptotic power-law index in the test-particle picture is *soft* (i.e.,  $s > 4$ ). This means that it is possible to consider a Lorentz factor above which the test-particle approximation is valid, because the energy density in the remaining accelerated particles is indeed small. Nevertheless, a strong nonlinear effect can be exerted by particles of lower energies, whose mean free path to scattering is comparable to the size of internal structures in the shock transition [Ellison and Double 2002].

In order to understand how a collisionless, relativistic shock can form, it is necessary to identify a suitable instability which can lead to dissipation in the nonlinear regime. Currently, the most promising approach to this problem considers the nonlinear development of the Weibel instability [Medvedev and Loeb 1999, Yang *et al.* 1994, 1993], which generates downstream magnetic field perpendicular to the streaming motion of the plasma i.e., in the plane of the incipient shock. Particle-in-cell simulations of this situation have been performed [Jaroschek *et al.* 2005, Nishikawa *et al.* 2003, Silva *et al.* 2003] suggesting that magnetic field can be generated with a strength  $\sigma_+$  of a few percent. (The magnetisation parameter  $\sigma_+$  is defined as the ratio of the magnetic energy density to twice the total enthalpy density (including rest mass) as measured in the downstream plasma rest frame). This is encouraging, since it is roughly the level implied by spectral modelling of GRB afterglows [Panaitescu and Kumar 2002]. However, it has so far not been possible to identify particles that partake in the first order Fermi process [Hededal *et al.* 2004], nor is the ultimate fate of the generated field fully understood [Medvedev *et al.* 2005].

The manner in which magnetic field is generated at the shock has a strong influence on the spectrum of accelerated particles. However, if we are interested only in high energy particles of long mean free path, the complex aspects of the problem can be by-passed: the power-law index predicted by the first-order Fermi mechanism can be calculated simply by modifying the shock jump conditions to account for the generated

field. To do this, consider time-averaged conditions, so that linear functions of the oscillating electromagnetic field vanish. The stress-energy tensor in the plasma frame is

$$T^{\mu\nu} = \left( w + \frac{B^2}{4\pi} \right) u^\mu u^\nu + \left( p + \frac{B^2}{8\pi} \right) g^{\mu\nu} - \frac{B^\mu B^\nu}{4\pi} \quad (3)$$

(for notation see Kirk and Duffy [1999]) and the last term on the right hand side does not contribute to the fluxes across the shock front if the magnetic field lies in the shock plane. As a result, the jump conditions are the same as those of an unmagnetised fluid, provided the magnetic enthalpy density  $B^2/4\pi$  and pressure  $B^2/8\pi$  are taken into account [Lyubarsky 2003]. For a relativistic gas, this gives an effective adiabatic index

$$\gamma_{\text{eff}} = \frac{4(1 + \sigma_+)}{(3 + \sigma_+)} \quad (4)$$

leading to an asymptotic compression ratio of  $1/(\gamma_{\text{eff}} - 1)$  and a relative speed of the upstream medium with respect to the downstream medium corresponding to the Lorentz factor  $\Gamma_{\text{rel}} = \Gamma \sqrt{(2 - \gamma_{\text{eff}})/\gamma_{\text{eff}}}$ . As  $\sigma_+$  increases, the compression ratio of the shock decreases and the high-energy power-law softens, as shown in Fig. 1. If magnetic field amplification indeed saturates at  $\sigma_+ \sim 1\%$ , the asymptotic spectral index still remains close to 4.2.

## 4. RELATIVISTIC CURRENT SHEETS

The first order Fermi process at a collisionless, relativistic shock does not appear to produce spectra with  $s \lesssim 4$ , so that an additional mechanism is required in many sources. Since this mechanism tends to manifest itself at lower energies, it could also play the role of injecting particles into the Fermi I process. Possible candidate processes include acceleration by a velocity shear [Rieger and Duffy 2004, Stawarz and Ostrowski 2002], the maser mechanism of Hoshino *et al.* [1992] and the *destruction* of magnetic flux in the shock front [Lyubarsky 2003], as well as the second order Fermi process of acceleration by a turbulent wave spectrum [Virtanen and Vainio 2005]. Another possibility is acceleration at relativistic current sheets [Kirk 2004]. As well as its obvious importance in the process of flux destruction, this possibility is particularly attractive in view of the fact that field reversals of short length scale can be generated at relativistic shocks [Medvedev *et al.* 2005].

The current sheets at which reconnection and particle acceleration takes place in astrophysics are relativistic in two senses: Firstly, the magnetisation parameter,  $\sigma$  is large and the Alfvén speed  $v_A =$

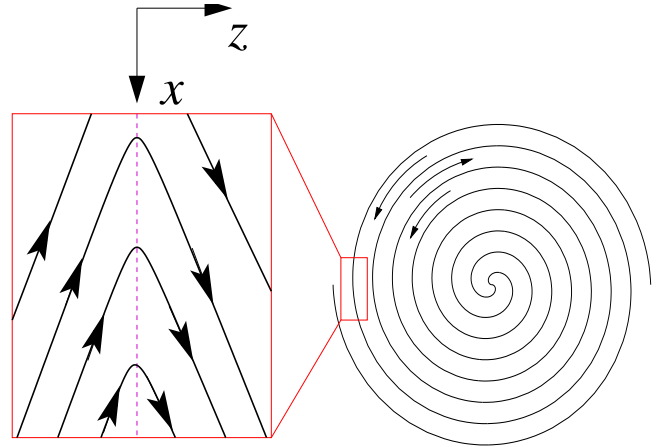
$c\sqrt{\sigma/(1+\sigma)}$  is close to  $c$ . Secondly, the geometry of the current sheet at which magnetic energy is dissipated and, hence, the field configuration, is dictated by a highly relativistic plasma flow. Particle acceleration depends crucially on both the magnetisation parameter and the field configuration.

The relativistic effects associated with a large magnetisation parameter are readily appreciated. On the other hand, the geometrical effects of a relativistic flow are more subtle. The situation is closely analogous to that of MHD shock fronts, which can be classified into “subluminal” and “superluminal” according to whether the speed of the intersection point of the magnetic field and the shock front is less or greater than  $c$  [Begelman and Kirk 1990, Drury 1983]. In each case, a Lorentz transformation enables the shock to be viewed from a reference frame in which it has a particularly simple configuration: either a de Hoffmann-Teller frame with zero electric field, or a frame in which the magnetic field is exactly perpendicular to the shock normal. In the case of a current sheet, the speed of the intersection point of the magnetic field lines and the sheet centre-line is important. If it is subluminal, a transformation to a de Hoffmann-Teller frame is possible, leading to the standard configuration for a nonrelativistic sheet [Büchner and Zelenyi 1989, Chen 1992]. Alternatively, for superluminal motion of the intersection point, which should be the rule for sheets in relativistic flows, a frame can be found in which the sheet is a true neutral sheet with no field lines linking through it. This is, in fact, the original configuration considered by Speiser [1965]. For a relativistic sheet, however, it is the *generic* case, rather than a very special singular one.

Most discussions of reconnection treat a Sweet-Parker or Petschek configuration in which the length of the current sheet in the average field direction determines the dissipation rate. This is also true for recent analytic treatments that are relativistic in the sense that the effects of large  $\sigma$  are included [Lyubarsky 2005, Lyutikov 2003, Lyutikov and Uzdensky 2002]. But the vanishing of  $B_z$  in the generic relativistic case has important implications, since it is the linking field that can eject particles from the sheet, making it crucial for the determination of the spectrum of accelerated particles, and, especially, the maximum permitted energy [Larrabee *et al.* 2003, Litvinenko 1999].

Relativistic current sheets, can extend over large distances along the field, depending on the nature of the boundary conditions. An example, drawn from the case of a striped pulsar wind [Coroniti 1990, Kirk and Skjæraasen 2003, Lyubarsky and Kirk 2001], is shown in Fig. 3. If we assume that reconnection leads on average to a stationary field configuration, then as the spiral pattern moves outwards, the linking field lines shown in the inset must move through the plasma at a speed sufficient to keep their average distance from the star constant. The striped

Figure 3: The striped pattern of a pulsar wind. A magnetic dipole embedded in the star at an oblique angle to the rotation axis introduces field lines of both polarities into the equatorial plane. The current sheet separating these regions is shown. In the inset, an almost planar portion of this sheet (dashed line) is shown, together with the magnetic field lines, assuming they undergo reconnection.



spiral pattern depicted in the figure is expected to be established well outside the light cylinder, defined to be at radius  $r = r_L$ , where the corotation speed reaches  $c$ . In this case, the magnetic chevrons, which must move a distance  $2\pi r$  in each rotation of the spiral pattern, have a superluminal speed equal to  $cr/r_L$ . Transformation to the frame in which the sheet is a true neutral sheet involves a small boost in the  $x$  direction, and the resulting configuration has a typical dimension in the azimuthal direction of  $\sim 2\pi r$ .

Particle acceleration in current sheets with finite linking field ( $B_z$ ) has been extensively investigated [Syrovatskii 1981]. But in the generic, relativistic, configuration, the linking field can play no role in ejecting particles from the sheet. Instead, acceleration is controlled by the finite extent of the sheet in latitude, i.e., in the direction parallel to the electric field ( $E_y$ ). This is limited not by the boundary conditions, but by local parameter values, as first described by Alfvén [1968]. Assuming the plasma consists of cold electrons and positrons, and that  $\sigma \gg 1$ , the maximum Lorentz factor  $\gamma_{\max}$  after acceleration is,

$$\gamma_{\max} = 2\sigma, \quad (5)$$

whereas a cold electron-proton plasma gives

$$\gamma_{\max} \approx \sigma \quad \text{for protons} \quad (6)$$

$$\gamma_{\max} \approx \sigma M/m \quad \text{for electrons,} \quad (7)$$

[Kirk 2004] with  $M$  and  $m$  the proton and electron masses, respectively. It is interesting to note that

in a plasma in which the magnetic field and particle *rest mass* are in rough equipartition ( $\sigma \approx 1$ ), the upper limit given by Eq. (7) coincides with that quoted by Lesch and Birk [1997]. However, this situation arises only in relativistic plasmas. In the interstellar medium, for example,  $\sigma \approx 10^{-9}$  or smaller, in which case the upper limit on the energy gain reduces to  $Mv_A^2$ . Standard estimates of the interstellar magnetic field and particle density ( $1 \mu\text{G}$ ,  $1 \text{ proton/cm}^3$ ) imply that electrons can be accelerated, at most, to only mildly relativistic energies. In this case, and in solar system applications, direct acceleration by the DC field may be masked by particle acceleration in the turbulence fed by reconnection or the associated shocks [Cargill 2001].

The picture sketched above applies only to quasi-steady current sheets. However, Zelenyi and Krasnosel'skikh [1979] have shown that relativistic current sheets are unstable to the growth of the tearing mode and other instabilities are also likely to operate (see, for example, Daughton [1999]). On scale lengths comparable to the sheet thickness an unsteady, oscillating component of  $B_z$  may be generated. Thus, locally, the nonrelativistic picture may be relevant to the micro-structure of the sheet, although not in its standard 2-dimensional stationary incarnations.

Particle-in-cell simulations can provide valuable insight here, provided they account for relativistic particle motion. Such simulations have been performed in 3D by Jaroschek *et al.* [2004] and Zenitani and Hoshino [2005], who noted the growth of corrugations in the current sheet in the direction of the electric field  $E_y$  and identified them as due to the relativistic drift kink instability. Jaroschek *et al.* [2004] found a very hard spectrum of energetic particles, that can be understood in terms of an “acceleration zone” near the sheet centre, in which the electric field exceeds the magnetic field. The escape rate from this zone is then approximated as the time taken by a particle to complete one quarter of a revolution around the linking component of the magnetic field [Zenitani and Hoshino 2001]. However, the role of the kink instability appears to place a relatively modest maximum energy limit on the acceleration process.

## 5. Summary

Although the details of the plasma physics remain obscure, simple kinematic considerations suggest that acceleration at shocks imprints a characteristic power-law index on the particle spectrum. In the case of relativistic shocks, it is  $p^{-4.2}$ , and seems not to be sensitive to nonlinear effects, or the effects of magnetic field generation at the level of  $\sigma_+ \sim \%$ .

A spectrum consistent with this prediction has been identified in a few objects, but observations also show

that acceleration into a much harder spectrum is needed at low energies. Current sheets are in principle capable of producing particles with such a spectrum, but a full understanding of the way they operate remains a challenging goal.

## References

- Achterberg, A., Y. A. Gallant, J. G. Kirk, and A. W. Guthmann, 2001, *MNRAS* **328**, 393.
- Alfvén, H., 1968, *J. Geophys. Res.* **73**, 4379.
- Baars, J. W. M., and A. P. Hartsuijker, 1972, *A&A* **17**, 172.
- Ballard, K. R., and A. F. Heavens, 1992, *MNRAS* **259**, 89.
- Bednarz, J., and M. Ostrowski, 1998, *Physical Review Letters* **80**, 3911.
- Begelman, M. C., and J. G. Kirk, 1990, *ApJ* **353**, 66.
- Bietenholz, M. F., and P. P. Kronberg, 1992, *ApJ* **393**, 206.
- Büchner, J., and L. M. Zelenyi, 1989, *J. Geophys. Res.* **94**, 11,821.
- Cargill, P. J., 2001, *Advances in Space Research* **26**, 1759.
- Casse, F., M. Lemoine, and G. Pelletier, 2002, *Phys. Rev. D* **65**, 023002.
- Chen, J., 1992, *J. Geophys. Res.* **97**, 15,011.
- Chevalier, R. A., 2000, *ApJL* **539**, L45.
- Coroniti, F. V., 1990, *ApJ* **349**, 538.
- Daughton, W., 1999, *Phys. Plasmas* **6**, 1329.
- Derishev, E. V., F. A. Aharonian, V. V. Kocharovskiy, and V. V. Kocharovskiy, 2003, *Phys. Rev. D* **68**, 043003.
- Drury, L. O., 1983, **46**, 973.
- Ellison, D. C., and G. P. Double, 2002, *Astroparticle Physics* **18**, 213.
- Hededal, C. B., T. Haugbølle, J. T. Frederiksen, and Å. Nordlund, 2004, *ApJL* **617**, L107.
- Hester, J. J., K. Mori, D. Burrows, J. S. Gallagher, J. R. Graham, M. Halverson, A. Kader, F. C. Michel, and P. Scowen, 2002, *ApJL* **577**, L49.
- Hoshino, M., J. Arons, Y. A. Gallant, and A. B. Langdon, 1992, *ApJ* **390**, 454.
- Jaroschek, C. H., H. Lesch, and R. A. Treumann, 2005, *ApJ* **618**, 822.
- Jaroschek, C. H., R. A. Treumann, H. Lesch, and M. Scholer, 2004, *Physics of Plasmas* **11**, 1151.
- Kennel, C. F., and F. V. Coroniti, 1984, *ApJ* **283**, 710.
- Kirk, J. G., 2004, *Physical Review Letters* **92**(18), 181101.
- Kirk, J. G., and P. Duffy, 1999, *Journal of Physics G Nuclear Physics* **25**, 163.
- Kirk, J. G., A. W. Guthmann, Y. A. Gallant, and A. Achterberg, 2000, *ApJ* **542**, 235.
- Kirk, J. G., and P. Schneider, 1987, *ApJ* **315**, 425.
- Kirk, J. G., and O. Skjæraasen, 2003, *ApJ* **591**, 366.

- Konopelko, A., A. Mastichiadis, J. Kirk, O. C. de Jager, and F. W. Stecker, 2003, *ApJ* **597**, 851.
- Krawczynski, H., P. S. Coppi, and F. Aharonian, 2002, *MNRAS* **336**, 721.
- Kundt, W., and E. Krotscheck, 1980, *A&A* **83**, 1.
- Larrabee, D. A., R. V. E. Lovelace, and M. M. Romanova, 2003, *ApJ* **586**, 72.
- Lemoine, M., and G. Pelletier, 2003, *ApJL* **589**, L73.
- Lesch, H., and G. T. Birk, 1997, *Astron. & Astrophys.* **324**, 461.
- Litvinenko, Y. E., 1999, *Astron. & Astrophys.* **349**, 685.
- Lyubarsky, Y., and J. G. Kirk, 2001, *ApJ* **547**, 437.
- Lyubarsky, Y. E., 2003, *MNRAS* **345**, 153.
- Lyubarsky, Y. E., 2005, *MNRAS* **358**, 113.
- Lyutikov, M., 2003, *MNRAS* **346**, 540.
- Lyutikov, M., and D. Uzdensky, 2002, *ApJ* **589**, 893.
- Massaro, E., G. Cusumano, M. Litterio, and T. Mineo, 2000, *A&A* **361**, 695.
- Mastichiadis, A., and J. G. Kirk, 1997, *A&A* **320**, 19.
- Medvedev, M. V., M. Fiore, R. A. Fonseca, L. O. Silva, and W. B. Mori, 2005, *ApJL* **618**, L75.
- Medvedev, M. V., and A. Loeb, 1999, *ApJ* **526**, 697.
- Moran, L., S. Mereghetti, D. Götz, L. Hanlon, A. von Kienlin, B. McBreen, A. Tiengo, R. Preece, O. R. Williams, K. Bennett, R. M. Kippen, S. McBreen, *et al.*, 2005, *A&A* **432**, 467.
- Nishikawa, K.-I., P. Hardee, G. Richardson, R. Preece, H. Sol, and G. J. Fishman, 2003, *ApJ* **595**, 555.
- Ostrowski, M., 1993, *MNRAS* **264**, 248.
- Ostrowski, M., and J. Bednarz, 2002, *Astron. & Astrophys.* **394**, 1141.
- Panaitescu, A., and P. Kumar, 2002, *ApJ* **571**, 779.
- Piran, T., 2005, *Reviews of Modern Physics* **76**, 1143.
- Rees, M. J., and J. E. Gunn, 1974, *MNRAS* **167**, 1.
- Rieger, F. M., and P. Duffy, 2004, *ApJ* **617**, 155.
- Sambruna, R. M., L. Maraschi, and C. M. Urry, 1996, *ApJ* **463**, 444.
- Silva, L. O., R. A. Fonseca, J. W. Tonge, J. M. Dawson, W. B. Mori, and M. V. Medvedev, 2003, *ApJL* **596**, L121.
- Speiser, T. W., 1965, *J. Geophys. Res.* **70**, 4219.
- Stawarz, L., and M. Ostrowski, 2002, *ApJ* **578**, 763.
- Stern, B. E., 2003, *MNRAS* **345**, 590.
- Syrovatskii, S. I., 1981, *Ann. Rev. Astron. Astrophys.* **19**, 163.
- Tavecchio, F., L. Maraschi, G. Ghisellini, A. Celotti, L. Chiappetti, A. Comastri, G. Fossati, P. Grandi, E. Pian, G. Tagliaferri, A. Treves, and R. Sambruna, 2002, *ApJ* **575**, 137.
- Virtanen, J. J. P., and R. Vainio, 2005, *ApJ* **621**, 313.
- Weiler, K. W., and N. Panagia, 1978, *A&A* **70**, 419.
- Yang, T.-Y. B., J. Arons, and A. B. Langdon, 1994, *Physics of Plasmas* **1**, 3059.
- Yang, T.-Y. B., Y. Gallant, J. Arons, and A. B. Langdon, 1993, *Physics of Fluids B* **5**, 3369.
- Young, A., L. Rudnick, D. Katz, and T. DeLaney, 2005, in *astro-ph/0502557*.
- Zelenyi, L. M., and V. V. Krasnosel'skikh, 1979, *Sov Phys A J* **56**, 819.
- Zenitani, S., and M. Hoshino, 2001, *ApJ* **562**, L63.
- Zenitani, S., and M. Hoshino, 2005, *ApJL* **618**, L111.